The influence of trace water concentration on iron oxide nanoparticle size†

Janet E. Macdonald,[a] Christopher J. Brooks[b] and Jonathan G. C. Veinot*[a]

Received (in Cambridge, UK) 7th April 2008, Accepted 14th May 2008
First published as an Advance Article on the web 19th June 2008
DOI: 10.1039/b805715j

The size of iron oxide nanoparticles, prepared from the thermal decomposition of $Fe(CO)_5$ in a high boiling solvent in the presence of oleic acid, is affected by water concentration, giving particles from sizes of 5.6 nm to as low as 2.2 nm.

The size control of near monodisperse iron and iron oxide nanoparticles synthesized from the thermal decomposition of $Fe(CO)_5$ in high boiling solvents and surfactants is well established. However, the processes associated with $Fe(CO)_5$ decomposition and subsequent particle formation are extremely complex and ill-understood.[1,2] Many factors, such as solvent and surfactant choice,[3–5] concentration ratios,[6] reaction times[4,7] and temperature[4] have been shown to play important roles. Even so, not all of the impacting factors have been identified. Recently, several research groups have attempted to separate and understand these factors in order to tailor particle size. Despite many modes of control, most studies have achieved sizes in the 3–20 nm range[2,8] and very few have shown particles with average diameters below 4 nm.[4,9] The most recent foci for attaining size control have been methods aimed at the separation of nucleation from growth processes.[7,10] As described by the LaMer model, growth onto existing particles is thermodynamically favourable, yet nucleation is kinetically favoured when the concentration of the active species involved in nucleation is high.[11–13] By extension, there are two general modes of attack for achieving small particles, namely increasing the number of nucleation events or inhibiting growth on the nucleated particles.

The latter has been studied by using surfactants that interact strongly with particle surfaces to inhibit growth. Weakly binding surfactants, such as oleylamine, give larger particles.[14,15] A combination of trioctylphosphine and trioctylphosphine oxide has been shown to give 3 nm particles.[8,9] Oleic acid and other long chain carboxylic acids are the most commonly used surfactants for obtaining some of the smallest monodisperse particles reported for the thermal decompositions of $Fe(CO)_5$ in high boiling solvents.[4,7] Oleic acid and oleate salts under varying synthetic conditions yield monodisperse particles in the 4–22 nm range.[3,16,17] However, Hyeon *et al*. have shown that increasing the oleic acid : $Fe(CO)_5$ ratio counter-intuitively increases particle size. This has been attributed to oleic acid binding the reactive species as iron oleate complexes and inhibiting nucleation events.[17] This counteracts the achievements of inhibiting growth.

In order to increase nucleation events, in essence some method should be developed to achieve rapid decomposition of $Fe(CO)_5$. Hyeon *et al*. have described nucleation as resulting from $Fe(CO)_5$ decomposition and growth occurring from the more stable iron oleate complexes that are created *in situ* or by subsequent addition.[10,16] $Fe(CO)_5$ decomposition can be aided by increasing reaction temperatures,[4] but nucleation is inhibited by the formation of iron oleate complexes at high temperatures. One of the earliest reported syntheses of monodisperse iron/iron oxide nanoparticles by thermal decomposition of $Fe(CO)_5$ used polymers as "surfactants" which were shown to catalyze the decomposition. Despite the catalysis, the smallest particle sizes reported were 6 nm.[5]

Here, we report evidence that water promotes the decomposition of $Fe(CO)_5$ to increase nucleation events and decreases particle size down to 2.2 nm and, as such, is an important factor in determining the particle size.

Particles were synthesized from the thermal decomposition of $Fe(CO)_5$ in oleic acid and benzyl ether as outlined in Supporting Information.† The decomposition of $Fe(CO)_5$ in high boiling solvents gives Fe(0) nanoparticles,[17] and

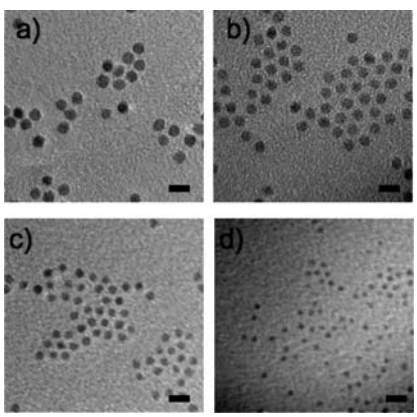

Fig. 1 Brightfield TEM images of iron oxide nanoparticles synthesized from the thermal decomposition of $Fe(CO)_5$ in benzyl ether and oleic acid (bar = 10 nm): (a) 101 ppm H_2O, particle diameters = 5.6 ± 0.5 nm; (b) 181 ppm H_2O, 4.9 ± 0.6 nm; (c) 657 ppm H_2O, 3.5 ± 0.4 nm; (d) 1590 ppm H_2O, 2.2 ± 0.4 nm.

[a] *Department of Chemistry, University of Alberta, Edmonton, Alberta, Canada. E-mail: jveinot@ualberta.ca; Fax: +1 (780) 492-8231; Tel: +1 (780) 492-7206*
[b] *Honda Research Institute USA, Inc., 1381 Kinnear Rd, Suite 116, Columbus, Ohio, USA*

† Electronic supplementary information (ESI) available: Additional experimental details, instrument specifications and statistical analysis of the data sets. See DOI: 10.1039/b805715j

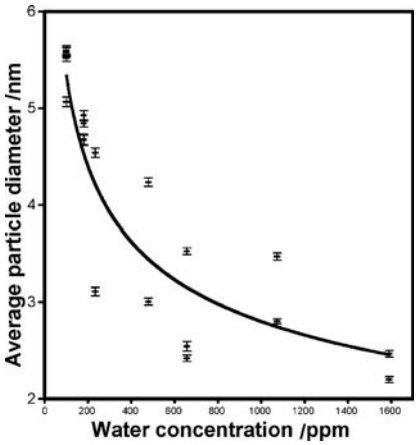

Fig. 2 The effect of water concentration on the average particle diameter in the thermal decomposition of $Fe(CO)_5$ to give iron oxide nanoparticles. Error bars are the standard error of the mean to highlight the differences in samples at the same water concentration. A curve is presented to guide the eye.

subsequent oxidation in ambient conditions gives crystalline γ-Fe_2O_3 nanoparticles[10] (Supporting Information†).

A distinctive trend relating particle size and initial water concentration was observed (Fig. 1 and Fig. 2). ANalysis Of VAriation (ANOVA) between the different water concentrations indicated the groups are statistically different at more than 99.999% confidence. Tukey's test for multiple comparisons over the different water concentrations indicates a statistically significant decrease in particle size with water concentration (Supporting Information†). With a water-saturated solution ($\sim$1600 ppm), average particle sizes were as low as 2.2 nm. At much lower concentrations of water ($\sim$100 ppm), average particle sizes were as large as 5.6 nm using otherwise identical reaction conditions. The standard deviations of the particle sizes for each data set were typically below 0.6 nm (see Supporting Information†).

Several explanations for this trend were dismissed based on literature precedent. It was possible that water was behaving as a base, deprotonating the oleic acid to oleate making it a more strongly binding surfactant. However, the addition of other bases, such as short chain amines, gave larger particles.[3] Equally, the addition of oxidants into the reaction mixture, another possible role for the water, also gave larger particles.[17]

Instead we propose that the water becomes intimately involved in the decomposition of $Fe(CO)_5$ to afford a more rapid decomposition and thereby increases nucleation events.

$Fe(CO)_5$ is a well studied model catalyst for the water-gas-shift reaction outlined in (1),

$$H_2O + CO \xrightarrow{Fe(CO)_5} H_2 + CO_2 \qquad (1)$$

The activation energy for the catalyzed reaction in (1) has been measured to be 22 kcal mol^{-1} in water–methanol[18] and 19 kcal mol^{-1} in the gas phase.[19] The rate-determining step is the initial addition of water, loss of a proton and insertion to form $Fe(CO)_4COOH^-$.[18] Without CO overpressure, decarbonylation is rapid and it is not rate-determining in the decomposition of $Fe(CO)_5$.[19] Indeed, the further loss of CO from the

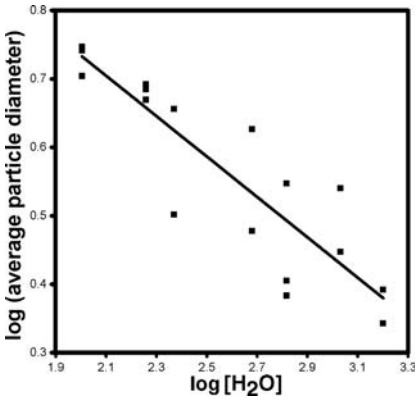

Fig. 3 Log–log plot of average particle diameter *versus* water concentration.

catalyst to form polynuclear iron complexes has long been known.[19,20]

The rate-determining step for $Fe(CO)_5$ decomposition in the absence of water-gas-shift conditions is the first decarbonylation. This process has an activation energy nearly twice that of the water-gas-shift reaction at 40 kcal mol^{-1}.[21] Therefore, the presence of water lowers the activation energy for the decomposition of $Fe(CO)_5$ by nearly a factor of 2. Since the rate of reaction is exponentially related to the negative of activation energy by the Arrhenius equation,[22] this lowering of the activation energy markedly increases the decomposition rate to afford a higher concentration of the unidentified active species for particle formation. This, in turn, leads to more nucleation events and decreased particle size.

A log–log plot of the data (Fig. 3) gives a linear trend with an equation:

$$\log d = -0.30 \log [H_2O] + 1.3 \; R^2 = 0.8013 \qquad (2)$$

where d is the average particle diameter. The R^2 of 0.80 indicates a strong correlation between the two variables. The value is a result of the scatter in the plot (the source of which will be discussed shortly) around the underlying linear trend.[23] The relationship can be expressed as:

$$d = 21[H_2O]^{-0.30} \qquad (3)$$

A physical interpretation of this result is not straightforward and requires a theoretical understanding of the relationship between particle volume, diameter and nucleation sites. Since the amount of $Fe(CO)_5$ in each reaction is constant, it can be assumed the total amount of iron is the same for every sample. Therefore the total volume, V_{tot}, of iron oxide is constant and may be expressed as the sum of all of the spherical particle volumes:

$$V_{tot} = \sum_{n=1}^{n} \tfrac{4}{3}\pi \left(\frac{d_n}{2}\right)^3 \qquad (4)$$

where n is the number of particles. Assuming our samples are monodisperse (*i.e.*, the diameters are equal), eqn (4) simplifies to:

$$V_{tot} = n\tfrac{4}{3}\pi \left(\frac{d}{2}\right)^3 \qquad (5)$$

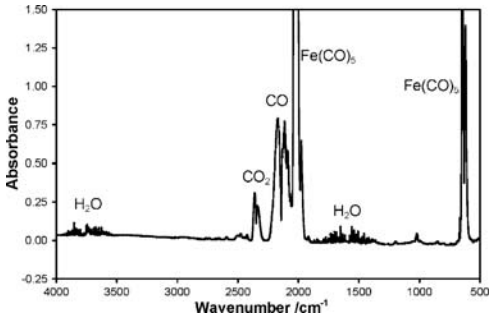

Fig. 4 FT-IR of the gas released from the thermal decomposition of $Fe(CO)_5$ in benzyl ether and oleic acid. Peaks indicative of $Fe(CO)_5$ are off-scale to allow visualization of the other components.

Rearrangement gives:

$$d = \left(\frac{6V_{\text{tot}}}{\pi}\right)^{\frac{1}{3}} n^{-\frac{1}{3}} \quad (6)$$

Using our hypothesis that water is intimately involved in nucleation and the concentration of water is directly proportional to the number of nuclei formed, a relationship is developed which describes the experimental results. Collecting constants as k, a theoretical relationship of:

$$d = k[H_2O]^{-\frac{1}{3}} \quad (7)$$

results, which is consistent with our experimental exponential dependency of −0.30 (3). This further supports the hypothesis that water is involved in nucleation.

To confirm water-gas-shift processes were indeed occurring, the gases emanating from the reaction were collected and analyzed by gas phase Fourier transform infrared spectroscopy (FT-IR) (Fig. 4). Ambient CO_2 was minimized and subtracted from the spectrum. FT-IR analysis confirmed four gases released from the reaction solution: CO (R and S rotational bands at 2170 and 2115 cm^{-1}), $Fe(CO)_5$ (11 bands between 2002–2041, 644, 619 cm^{-1}), CO_2 (R and S rotational bands of the asymmetric stretch at 2360 and 2339 cm^{-1}) and water vapour (asymmetric stretching modes between 3500–3800 cm^{-1}, bending modes between 1500 and 1900 cm^{-1}).

The presence of CO is consistent with the decomposition of $Fe(CO)_5$ and the presence of CO_2 confirms water-gas-shift reactions occur despite the acidic conditions.[19] The other gas produced by the water-gas-shift reaction, H_2, was not identified as it is not IR active. As the reaction temperatures were well above the boiling points of $Fe(CO)_5$ (bp 103 °C)[2] and water, the presence of a very strong absorbance from $Fe(CO)_5$ and a weaker contribution from H_2O is not surprising. However, their presence indicates the concentrations of these two species in solution are somewhat variable. For this reason, every effort was made to ensure consistent heating rates and identical reaction apparatus were employed so that these effects would be as systematic as possible.

Consistent heating rates and resting temperatures were vital to the observation of the present trend (Fig. 2). Compared to the ~1 h heating time to reach ~200 °C (Fig. 2), when heating took at least twice as long to reach the resting temperature much larger particles were obtained: 4.4 ± 0.5 nm at initially 1073 ppm H_2O and 4.6 ± 0.5 nm at initially 1590 ppm H_2O. Slower heating allows more substantial evaporation of H_2O, reducing the influence of water-gas-shift chemistry for $Fe(CO)_5$ decomposition.

This effect of heating rates on the particle diameter is the likely cause of the observed scatter in the plot (Fig. 2). In repetitive experiments at the same water concentrations ANOVA revealed the samples were indeed statistically different (Supporting Information†, visualized as error bars in Fig. 2). Small variations in heating rates resulted in subtle changes in the H_2O concentration causing scatter in the plot.

The present findings illuminate the influence of water concentration on particle size in the decomposition of $Fe(CO)_5$ to give near monodisperse nanoparticles of iron oxide. Average particle sizes were observed to range from 5.6 nm down to 2.2 nm by simply changing the water concentration.

Funding for this research came from Honda Research Institute, Inc. and the Natural Sciences and Engineering Research Council of Canada. We thank the University of Alberta Department of Physics for the use of their TEM and to Nancy Macdonald, Makedonka D. Gulcev and Prof. Charles S. Wong for their useful advice on statistical analysis. Thanks also to Wayne Moffat, Ryan Lister, Victoria Russell and Kristina Boates.

Notes and references

1 R. Psaro, A. Fusi, R. Ugo, J. M. Basset, A. K. Smith and F. Hugues, *J. Mol. Catal.*, 1980, **7**, 511–522.
2 D. L. Huber, *Small*, 2005, **1**, 482–501.
3 M. V. Kovalenko, M. I. Bodnarchuk, R. T. Lechner, G. Hesser, F. Schaffler and W. Heiss, *J. Am. Chem. Soc.*, 2007, **129**, 6352–6353.
4 X. W. Teng and H. Yang, *J. Mater. Chem.*, 2004, **14**, 774–779.
5 T. W. Smith and D. Wychick, *J. Phys. Chem.*, 1980, **84**, 1621–1629.
6 *The Merck Index*, Merck and Co., Whitehouse Station, NJ, 13th edn, 2001, p. 181.
7 M. F. Casula, Y. W. Jun, D. J. Zaziski, E. M. Chan, A. Corrias and A. P. Alivisatos, *J. Am. Chem. Soc.*, 2006, **128**, 1675–1682.
8 U. Jeong, X. W. Teng, Y. Wang, H. Yang and Y. N. Xia, *Adv. Mater.*, 2007, **19**, 33–60.
9 S. J. Park, S. Kim, S. Lee, Z. G. Khim, K. Char and T. Hyeon, *J. Am. Chem. Soc.*, 2000, **122**, 8581–8582.
10 J. Park, E. Lee, N. M. Hwang, M. S. Kang, S. C. Kim, Y. Hwang, J. G. Park, H. J. Noh, J. Y. Kini, J. H. Park and T. Hyeon, *Angew. Chem., Int. Ed.*, 2005, **44**, 2872–2877.
11 V. K. Lamer and R. H. Dinegar, *J. Am. Chem. Soc.*, 1950, **72**, 4847–4854.
12 T. Sugimoto, *J. Colloid Interface Sci.*, 2007, **309**, 106–118.
13 A. G. Roca, M. P. Morales and C. J. Serna, *IEEE Trans. Magn.*, 2006, **42**, 3025–3029.
14 S. Peng, C. Wang, J. Xie and S. H. Sun, *J. Am. Chem. Soc.*, 2006, **128**, 10676–10677.
15 J. W. Cheon, N. J. Kang, S. M. Lee, J. H. Lee, J. H. Yoon and S. J. Oh, *J. Am. Chem. Soc.*, 2004, **126**, 1950–1951.
16 T. Hyeon, *Chem. Commun.*, 2003, 927–934.
17 T. Hyeon, S. S. Lee, J. Park, Y. Chung and H. Bin Na, *J. Am. Chem. Soc.*, 2001, **123**, 12798–12801.
18 A. D. King, R. B. King and D. B. Yang, *J. Am. Chem. Soc.*, 1980, **102**, 1028–1032.
19 L. S. Sunderlin and R. R. Squires, *J. Am. Chem. Soc.*, 1993, **115**, 337–343.
20 W. Hieber and H. Vetter, *Z. Anorg. Allg. Chem.*, 1933, **212**, 145–168.
21 K. E. Lewis, D. M. Golden and G. P. Smith, *J. Am. Chem. Soc.*, 1984, **106**, 3905–3912.
22 R. B. Jordan, *Reaction Mechanisms of Inorganic and Organometallic Systems*, Oxford University Press, New York, 2nd edn, 1998, p. 15.
23 D. G. Altman, *Practical Statistics for Medical Research*, Chapman and Hall, New York, 1991, pp. 278–279, 308–309.